Journal of Biomedical Materials Research Part A

Influence of Nanoparticle-embedded Polymeric Surfaces on Cellular Adhesion, Proliferation and Differentiation

Journal:	*Journal of Biomedical Materials Research: Part A*
Manuscript ID:	JBMR-A-13-0342.R2
Wiley - Manuscript type:	Original Article
Date Submitted by the Author:	n/a
Complete List of Authors:	Ventrelli, Letizia; Istituto Italiano di Tecnologia, Center for Micro-BioRobotics @SSSA; Scuola Superiore Sant'Anna, The Biorobotics Institute Fujie, Toshinori; Istituto Italiano di Tecnologia, Center for Micro-BioRobotics @SSSA; Tohoku University, WPI-Advanced Institute for Materials Research Del Turco, Serena; CNR, Istituto di Fisiologia Clinica Basta, Giuseppina; CNR, Istituto di Fisiologia Clinica Mazzolai, Barbara; Istituto Italiano di Tecnologia, Center for Micro-BioRobotics @SSSA Mattoli, Virgilio; Istituto Italiano di Tecnologia, Center for Micro-BioRobotics @SSSA
Keywords:	Cellular scaffolds, Cardiac tissue engineering, Ultra-thin films, Magnetic nanoparticles, Surface roughness

Influence of Nanoparticle-embedded Polymeric Surfaces on Cellular Adhesion, Proliferation and Differentiation

Letizia Ventrelli [a,b,*], Toshinori Fujie [a,c], Serena Del Turco [d], Giuseppina Basta[d], Barbara Mazzolai [a], Virgilio Mattoli [a,*]

[a] Center for Micro-BioRobotics @SSSA, Istituto Italiano di Tecnologia, Viale Rinaldo Piaggio, 34, 56025 Pontedera (PI), Italy

[b] The BioRobotics Institute, Scuola Superiore Sant'Anna, Polo Sant'Anna Valdera, Viale Rinaldo Piaggio, 34, 56025 Pontedera (PI), Italy

[c] WPI-Advanced Institute for Materials Research (WPI-AIMR), Tohoku University, 2-1-1 Katahira, Aoba-ku, Sendai, 980-8577, Japan

[d] Istituto di Fisiologia Clinica, CNR, Area di Ricerca San Cataldo, Via Moruzzi, 1, 56124 Pisa, Italy

* To whom all correspondence should be addressed:

Letizia Ventrelli, M.Sc., Ph.D. candidate; Virgilio Mattoli, Ph.D.

Center for Micro-BioRobotics@SSSA, Istituto Italiano di Tecnologia

Viale Rinaldo Piaggio, 34, 56025 Pontedera (PI), Italy

Tel: +39-050-883414. Fax: +39-050-883101. E-mail address: l.ventrelli@sssup.it; virgilio.mattoli@iit.it

Influence of Nanoparticle-embedded Polymeric Surfaces on Cellular Adhesion, Proliferation and Differentiation

Abstract

The development of functional substrates to direct cellular organization is important for biomedical applications such as regenerative medicine and biorobotics. In this study, we prepared freestanding polymeric ultra-thin films (nanofilms) consisting of poly(lactic acid) (PLA) and magnetic nanoparticles (MNPs), and evaluated the effects of their surface properties on the organization of cardiac-like rat myoblasts (H9c2). We changed surface properties of the PLA nanofilms (i.e. roughness and wettability) as a function of MNPs concentration. We found that the incorporation of MNPs into the nanofilms enhanced both proliferation and adhesion of H9c2 cells. Through the morphological assessment of the differentiated H9c2 cells, we also found that the presence of MNPs significantly increased the fusion index and the surface area of myotubes. In conclusion, the embedding of MNPs is a simple method to tailor the physicochemical properties of the polymeric nanofilms, yet it is an effective approach to enhance the cellular morphogenesis in the field of cardiac tissue engineering for regenerative medicine and biorobotics applications.

Keywords

Cellular scaffolds, Cardiac tissue engineering, Ultra-thin films (nanofilms), Magnetic nanoparticles, Surface roughness.

INTRODUCTION

The development of functional biomaterials is of particular interest in many biomedical applications, such as the fields of regenerative medicine and tissue engineering. Accordingly, engineered scaffolds should allow cells to attach, grow, keep their viability and, if necessary, be transplanted into a specific wounded area of the human body.[1-4] In order to obtain a successful engineered biomaterial acting as a substrate for tissue regeneration, the following main requirements are demanded:[5] *(i)* biocompatibility with host tissue; *(ii)* safe biodegradability; *(iii)* specific morphological, mechanical and chemical properties promoting suitable interactions with cells (e.g. adhesion and migration). In addition to this, the fabrication process should be easy, controlled and reproducible.

Among these requirements, when coupling desired cell type with a flexible substrate, the control of its surface morphology has to be considered and deeply studied. In fact, it has been demonstrated that cellular events (adhesion, proliferation, migration and differentiation) are sensitive to and can be affected by the surface properties of the material.[6-8] Concerning the first cellular event occurring when there is contact between the cells and the substrate, Raffa *et al.* proved that surfaces with nanometer-scale topography directed the PC12 pheochromocytoma cells adhesion.[9] Instead, Washburn *et al.* reported that the proliferation of MC3T3-E1 osteoblastic cell was sensitive to the nanometer-scale roughness of the polymeric materials.[10] Also, the differentiation process can be affected by altering both the surface and the bulk structure of the materials.[11]

In the last decade, many tissue engineering technologies have been developed in order to direct the cellular growth as well as their morphogenesis. In addition, several strategies have been created to use biomaterials as functional substrates for cell delivery. Among different tissue engineering applications, cardiac tissue engineering (CTE) represents the starting point of our study. The aim of CTE is to repair or regenerate a damaged section of the heart, and it comprises different issues; in particular, the search for alternative cell delivery techniques is continuously being carried out.[5] For example, Sung's group developed an alternative method for CTE, based on the fabrication of fragmented cell sheets, by using thermo-responsive methylcellulose (MC) hydrogel coated on tissue culture polystyrene (TCPS) dishes.[12] Then, Yeh *et al.* prepared and transplanted into the peri-ischemic area of a rat model cell sheet fragments seeded with human amniotic fluid stem cells (hAFSCs).[13] The results showed the capability of hAFSCs to differentiate into cardiomyocyte-like cells as well as significant improvements in the cardiac function. Another tissue engineering strategy is based on tissue-bioengineered patches, basically constructed from both biological and synthetic scaffolds laden with a cell-culture system.[14] For example, Piao *et al.* used rat bone marrow-derived mononuclear cells (BMMNCs) seeded onto a poly-glycolide-*co*-caprolactone (PGCL) scaffold; after its implantation into the epicardial surface of a rat myocardial infarction model, migration and differentiation into cardiomyocytes were found out.[15]

Recently, we developed biocompatible and biodegradable polymeric ultra-thin films (referred as "nanofilms") as further choice for promoting cell growth, thus acting as organized cellular substrate. Nanofilms are recently investigated as a new category of quasi-two dimensional polymeric biomaterial; their main features are freestanding structures with the thickness of tens to hundreds of nanometers, several square centimeters of surface area, and extremely high flexibility.[16] Such nanofilms can be prepared simply through the spin coating assisted deposition by using a wide variety of polymers such as polysaccharides, extra-cellular matrix proteins and synthetic biodegradable polyesters.[17] In this way, biocompatible nanofilms are obtained and used for several biomedical applications in minimally invasive surgery (such as sealing operations in tissue-defect repair),[18,19] in skincare applications as plasters,[16] as surface coatings for implantable devices or prosthesis (bone implants and endovascular stents),[20,35,36] as drug-delivery systems,[26] and many other applications[21,22,42]. All these studies therefore suggest that nanofilms may also work as engineered cellular scaffolds in the field of tissue regeneration. For instance, we developed polymeric nanofilms bearing C2C12 skeletal muscle cells, suggesting their application as an artificial cellular matrix for bio-hybrid contractile systems.[23] On the other hand, we fabricated nanofilms cultured with different types of cells (among which mesenchymal stem cells) in order to design a cell delivery platform for bone or tendon repair and healing, evaluating their biocompatibility and both adhesion and proliferation activities.[24] Quite recently, we also demonstrated the mechanobiological control of cell adhesion properties by culturing H9c2 cardiac myoblasts on freestanding nanofilms which were coupled with mechanically rigid materials.[25]

Therefore, motivated by the necessity to develop flexible substrates delivering specific cells to the diseased tissue for CTE applications, we fabricated poly(lactic acid) (PLA) nanofilms functionalized with magnetic nanoparticles (MNPs) as remote-controllable cellular scaffolds. In our previous studies, we encapsulated MNPs within polymeric nanofilms and demonstrated the remote control of such freestanding magnetic nanofilms by means of an external magnetic field, which could allow the precise positioning of the nanofilm inside the body (i.e. the infarcted heart).[26] In this regard, we employed a cardiac-like rat cell line (H9c2), which is a subclone of the original clonal cell line derived from the embryonic BDIX rat heart tissue.[37] This cell line has been widely used as an experimental model of cardiomyocytes, and it has been studied for its sensitiveness to substrates topography. In fact, it was demonstrated that the adhesion, proliferation and differentiation rates of H9c2 myoblasts are strongly affected by the matrix properties.[38,39] Combining this behavior with the importance of magnetic nanofilms,[27] we focused on the effects of their surface properties on the biological activity of H9c2 cells. In this study, we evaluated the surface properties (i.e. thickness, roughness and wettability) of the magnetic PLA nanofilms as a function of different MNPs concentrations. Then, we assessed the cytocompatibility and proliferation of H9c2 on the magnetic nanofilms. Finally, we analyzed the influence of the surface properties of these substrates on the cellular morphogenesis in terms of adhesion and differentiation.

MATERIALS AND METHODS

Fabrication of magnetic polymeric nanofilms. Single layer magnetic nanofilms were fabricated by spin-coated assisted deposition with the procedure described as follows. Briefly, new silicon wafers (SiO_2 substrates, Si-Mat Silicon Materials, Kaufering, Germany), used as substrates for film deposition, were cut into 4 cm^2 by a diamond blade, cleaned for 10 min with the *Piranha solution* (typical mixture 3:1 concentrated sulfuric acid and hydrogen peroxide) and then rinsed with deionized (DI) water in order to remove dust or other impurities. A poly(lactic acid) (PLA) (Mw ~60,000, Sigma-Aldrich Co.) solution (20 mg/mL in chloroform) containing iron oxide nanoparticles (referred as MNPs) (polymer-coated EMG1300, nominal diameter of 10 nm, FerroTec Co., San Jose, CA) was deposited by a single step of spin coating (WS-650 spin processor, Laurell Technologies Corporation, North Wales, PA) on the silicon substrate at 4,000 rpm for 40 s. In this study, different magnetic nanofilms were prepared varying the concentration of MNPs in the PLA solution: 0 (used as control), 5, 10 and 15 mg/mL have been tested. In order to avoid contamination, all the preparation steps of magnetic nanofilms were performed in a class 10,000 clean room.

Surface characterization of magnetic polymeric nanofilms. Macroscopic optical images of the magnetic PLA nanofilms onto the silicon wafer were taken by using a Hirox KH-7700 digital microscope (Hirox Co Ltd., Tokyo, Japan) provided with a MX(G)-10C zoom lens and an OL-140II objective lens (magnification range from 140× up to 1,400×). Thickness, topography and surface roughness of the magnetic PLA nanofilms onto SiO_2 substrate were afterwards evaluated by Atomic Force Microscopy (AFM) (Veeco Innova Scanning Probe Microscope, Veeco Instruments Inc., Santa Barbara, CA) operating in tapping mode, using a RTESPA Al-coated silicon probe (Veeco Instruments Inc.) at a resonant frequency of 235-317 kHz. All the measurements were performed in air at room temperature (25°C). For thickness measurements, nanofilms were scratched through a thin blade and then scanned across the edge with a cross-sectional analysis (scan range of 20 μm), recording 64 × 64 samples. For roughness (root mean square, rms) measurements, the surface of nanofilms on the SiO_2 substrate was scanned in tapping mode over 5 μm × 5 μm area, collecting 512 × 512 samples and recording the topography, phase and amplitude channels. Then, the rms values were obtained from the topographical images. For both measurements, the resulting scanned images were examined using Gwyddion-free SPM data analysis software (http://gwiddion.net).[27]

In order to evaluate the hydrophobic nature of the magnetic PLA nanofilms for different MNPs concentrations, the water contact angle was estimated through the static sessile drop method. By means of a micropipette pointed vertically down, small DI water droplets (5 μL) were deposited onto the horizontal surface-air interface of the samples, and the corresponding profiles were captured by the Hirox KH-7700 digital microscope. All measurements were performed in air at room temperature (25°C). Through the ImageJ software for image analysis (free download from NIH, http://rsbweb.nih.gov/ij/), the water contact angle was calculated as the angle formed between the liquid/solid interface (the baseline of the drop) and the liquid/air interface (the tangent to the drop starting from the baseline).

H9c2 cell culture. H9c2 embryonic myocardium rat cells (CRL-1446, ATCC, Milano, Italy) were cultured in Dulbecco's modified Eagle's medium (DMEM) (ATCC) supplemented with 10% fetal bovine serum (FBS) (ATCC), 100 μg/mL gentamycin and 4 mM/L L-glutamine, and maintained in normal culture conditions (37°C, saturated humidity atmosphere at 95% air / 5% CO_2). Before reaching confluence, cells were still sub-cultured onto 25 cm^2 cell culture flasks. In this study, differentiation of H9c2 cells into myotubes was subsequently induced one day after cell seeding onto magnetic PLA nanofilms by replacing the culture medium from expansion to differentiation one; this last was composed of DMEM plus 100 μg/mL gentamycin, 4 mM/L L-glutamine, 1% FBS and 1% Insulin-Transferrin-Selenium (ITS) (I3146, Sigma, St Louis, MO). From the third day after the switching of the medium to the end point, cells were supplied with a second differentiation medium containing 0.25 μL/mL Aracytin (AraC) (purchased from Pfizer), in order to contrast a continuous cell proliferation at early stages of differentiation. Prior to cell seeding, sterilization of the magnetic nanofilms was performed by means of an UV rays treatment for 45 min. H9c2 cells were then seeded on the surface of each nanofilm at the same initial cell concentration (6×10^4 cells/mL) with the following procedure. Briefly, first of all cells were detached from the flask using a 0.05 wt% trypsin with phenol red solution; secondly, the aliquot was purified by centrifugation and suspended in the fresh culture medium. Finally, a tiny amount of the cell suspension (320 μL) was placed onto the surface of the samples and incubated for 30 min to allow H9c2 attachment. Additional culture medium was then added, and the samples were cultured under standard conditions for 24 h.

Proliferation assays: viability staining and DNA quantification. To assess the cytocompatibility of MNPs with H9c2 cells, cell proliferation on magnetic PLA nanofilms (seeding density of 6×10^4 cells/mL) was evaluated after 24 h of incubation by means of two tests.[25] Firstly, viability was qualitatively investigated with the LIVE/DEAD® Viability/Cytotoxicity Kit (Invitrogen Co., Carlsbad, CA). The kit contains calcein acetoxymethylester (calcein AM, 4 mM in anhydrous dimethyl sulfoxide) and ethidium homodimer-1 (EthD-1, 2 mM in dimethyl sulfoxide/water 1:4 v/v), and identifies live (green fluorescence) versus dead (red fluorescence) cells based on membrane integrity and esterase activity. In brief, after 24 h incubation, the culture medium was removed and the cell layers grown on the surface of nanofilms at different concentrations of MNPs (0, 5, 10 and 15 mg/mL) were rinsed with phosphate buffered saline (PBS) and treated for 10 min at 37°C with 2 μM/L calcein AM and 4 μM/L EthD-1. Cells were finally observed under an inverted fluorescent microscope (TE2000U, FITC-TRITC filters, Nikon Co., Tokyo, Japan) equipped with a cooled CCD camera (DS-5MC USB2, Nikon Co., Tokyo, Japan) and with NIS Elements Imaging Software.

Secondly, cell proliferation was also quantitatively evaluated assessing the DNA concentration after 24 h of incubation by means of a Quant-iT dsDNA PicoGreen kit (Invitrogen Co., Carlsbad, CA).[24] Briefly, after the removal of the culture medium from each well, 500 μL of DI water was added. Samples were thus frozen and defrosted twice obtaining the cell lysates, and then sonicated to allow the DNA to float into solution. Working buffer and PicoGreen dye solutions were prepared according to the manufacturer's instructions, added to a 96-well cell culture plate and then incubated in the dark at room temperature for 10 min. Finally, the fluorescence intensity from each sample was read in a fluorescence microplate reader (Victor3, PerkinElmer Inc., Waltham, MA) at 485 nm excitation and 535 nm emission.

Immunofluorescence of cytoskeletal actin. The influence of magnetic PLA nanofilms with different concentrations of MNPs (0, 5, 10 and 15 mg/mL) on H9c2 adhesion properties was determined. The cell adhesion area was measured using the actin staining as follows. In brief, cells grown on nanofilms (seeding density of 6×10^4 cells/mL) were fixed with a 4% paraformaldehyde (PFA) in PBS solution after 24 h of culture in the expansion medium[25], and subsequently permeabilized with 0.1% TritonX-100 in PBS; both treatments were performed for 15 min at room temperature. Cells were thus stained using Alexa Fluor® 594 phalloidin and Hoechst (Invitrogen Co., Carlsbad, CA), which identify the actin filaments with a green fluorescence and the single nuclei with a blue one, respectively, and visualized by the inverted fluorescent microscope. Finally, the cell adhesion area (average area/cell) was automatically measured using the ImageJ software.

Morphological assessments of differentiated cultures. In order to prove the potential influence and the effects of magnetic PLA nanofilms loaded with different MNPs concentrations on the differentiation process of H9c2, a morphological assessment of the cells was performed. For this purpose, a higher cell concentration (4×10^5 cells/mL) was used, and after 24 h of cells seeding culture medium was switched from the proliferating one to the differentiating one as described in the Section "*H9c2 cell culture*". Therefore, two different analysis were realized on H9c2 cells. In the first one, the morphological appearance of cells as well as their arrangement and fusion[28] was qualitatively assessed after 7 days of differentiation. Immunofluorescence stainings of nuclei and cytoskeletal actin were performed as reported in the Section

"*Immunofluorescence of cytoskeletal actin*". In the second analysis, a couple of parameters[29] was evaluated from the previously collected pictures by using ImageJ software, in order to quantify the further differentiation property. Then, the fusion index (total number of nuclei in myotubes (≥ 2 nuclei)/ total number of counted nuclei) and the surface area of the myotubes (total area of differentiated cells measured over the entire image) were calculated.

Statistical analysis. All the experimental data from each quantitative study are presented as mean values (MEAN) ± standard deviation (STDEV) of the indicated numbers of determinations (N). Statistical comparisons were conducted by twos between both nonmagnetic and the given MNPs-loaded groups and all magnetic groups having different MNPs concentrations. Multiple comparisons were performed by Analysis of Variance (ANOVA) followed by a post-hoc test (Bonferroni test). Values of $P < 0.05$ were considered statistically significant.

RESULTS AND DISCUSSION

Surface properties of magnetic polymeric nanofilms. A qualitative analysis of the surface properties of magnetic nanofilms was carried out by a digital optical microscope, showing homogeneous surfaces without holes, scratching or other defects. From a preliminary quality assessment, patterns of structural colors were found out suggesting a color modulation all over the film surface. As described by Taccola *et al.*, this phenomenon resulted from the microscopic modulation of the color due to a periodic topological variation of nanofilms thickness over the entire surface.[27] In detail, at low MNPs concentration (5 mg/mL), a homogeneous dispersion of small particles (black dot spots) was observed (Figure 1b, inset), whereas both single and aggregations (clusters) of MNPs were found at higher concentration (15 mg/mL) (Figure 1d, inset). The presence of these clusters (average size around 13 μm) is related to parameters such as PLA concentration and viscosity that influence the aggregation of small particles in the polymer-nanoparticles composite solution during the spin coating process.[27] Moreover, the fabrication procedure (with a specific spinning velocity and time) combined with a high mass fraction of MNPs could cause particles aggregations by short-range van der Waals dispersive interactions.[27]

Figure 1 about here

After the macroscopic observation, a microscopic characterization of the magnetic PLA nanofilms (i.e. surface roughness and thickness) was performed by AFM analysis for 5 different samples in order to quantify the influence of the MNPs concentration on the surface properties of nanofilms. By using a low scan range area, topography and roughness of the magnetic nanofilms were evaluated. Nanofilms without MNPs showed a flat surface (Figure 2a), whereas the ones with MNPs possessed monolayered particles (Figure 2b), which became clusters (Figure 2d) as the nanoparticles concentration increased from 5 to 15 mg/mL. These clusters formations were reflected to the surface roughness of the nanofilms, which increased with the increment of the MNPs concentration (Table 1).

Figure 2 about here

A complete characterization of the magnetic PLA nanofilms was provided by the measurement of their thickness. The thickness of nanofilms depends on several parameters, such as polymer concentrations, spinning conditions and the concentration of the MNPs.[30] In fact, the AFM scans confirmed that higher MNPs concentrations caused an increment of the nanofilm thickness due to the MNPs derived clusters formation. The obtained thicknesses were reported in Table 1. Therefore, the AFM analysis showed that the MNPs concentration affected both thickness and surface roughness of the nanofilms; in particular, the surface roughness is an important parameter able to direct the cellular morphogenesis (i.e. cell proliferation, adhesion and differentiation).[31]

To determine the superficial properties of the magnetic nanofilms, we also measured the water contact angles (Figure 3).

Figure 3 about here

The data reported in Table 1 showed that the water contact angle gradually increased with the increment of the MNPs concentration. Furthermore, the results obtained after a statistical analysis (data not shown) revealed significant differences in water contact angles of the nanofilms between with and without MNPs ($*p < 0.05$). However, magnetic nanofilms loaded with 15 mg/mL of MNPs versus 10 mg/mL exhibited a slight increment of the contact angle. We can therefore conclude that the embedding of growing MNPs concentrations inside the polymeric matrix led to an increase not only in nanofilms surface roughness but also in their hydrophobicity.

Table 1 about here

Effects of magnetic polymeric nanofilms on cell proliferation. Since the developed magnetic PLA nanofilms are intended to be applied in the field of CTE as cell delivery scaffolds, the insertion of these bio-scaffolds into the heart has to occur immediately after myocardial infarction in order to rapidly repair the damaged area.[5,34] For this purpose, the effect of the embedded MNPs on the cytocompatibility of H9c2 cells was evaluated at 24 h after their seeding on the nanofilms. The results obtained using the LIVE/DEAD® assay showed that cells were viable (green fluorescence) on each sample without showing significant apoptotic behavior (red fluorescence) (Figure 4). Thus, H9c2 has a capability to proliferate on the magnetic nanofilms independently from the MNPs concentration. Moreover, though the initial cellular seeding density was the same for all nanofilms, the density at 24 h on the magnetic nanofilms (Figure 4b-d) was much higher than the one on the control nanofilm (Figure 4a). The results found from the nanofilms AFM analysis (i.e. MNPs concentrations affecting the surface roughness of the films) and those from the early LIVE/DEAD® assay suggest the influence of substrates roughness due to the inclusion of MNPs on the enhanced H9c2 cell proliferation.

Figure 4 about here

In order to confirm further bioactivity, the qualitative LIVE/DEAD® assay was combined with the DNA quantitative assay. An increase in DNA level demonstrated the ability of H9c2 to proliferate on magnetic PLA nanofilms (Figure 5). An high significant difference (**$p < 0.001$) in DNA content between nanofilms with and without MNPs was obtained. Specifically, H9c2 cells cultured on substrates with 10 mg/mL of MNPs versus unloaded substrates exhibited an approximately three-fold increase in DNA content (**$p < 0.001$), while cells cultured on substrates with 15 mg/mL of MNPs exhibited a DNA increment (**$p < 0.001$) versus the unloaded samples but a slight decrement versus the ones loaded with 10 mg/mL of MNPs ($p = 0.015$).

Figure 5 about here

All together, the proliferation results suggested that, even if H9c2 cells were able to survive on all tested magnetic nanofilms in a concentration-dependent manner, a plateau in cell proliferation seemed to be reached at the highest (15 mg/mL) tested MNPs concentration.

As demonstrated in several studies found in literature, it is noteworthy that the cellular morphogenesis is sensitive to variations in nanometer-scale substrates topography; in particular, nanoroughness has found to be capable to influence cell proliferation[23,31,43]. Furthermore, it has been demonstrated that H9c2 cells (i.e. H9c2 proliferation) are sensitive to substrates topography[38]. Therefore, the results obtained from the characterization of magnetic PLA nanofilms through the AFM investigation and those achieved from the studies on cell proliferation (i.e. good cell viability and the increment in DNA content) highlighted that the MNPs concentration can affect the capability of these substrates to support H9c2 cells growth.

Nanofilms effects on cell adhesion properties. The assessment of cell adhesion properties on a substrate is important because it is the initial event occurring when there is contact between the cells and the substrate. As shown in Figure 6, the green fluorescence of the cytoskeleton illustrated that H9c2 cells attached to and spread on the nanofilms with a polygonal shape and well-defined actin filaments; in addition, it seemed that the number of adhered and spread cells has risen with the increase of the MNPs concentration (Figure 6a-d).

To quantify the above-observed results, the adhesion properties of H9c2 were evaluated by measuring the cell adhesion area as a function of the MNPs content. Figure 6e illustrates an increase of the adhesion area in case of nanofilms containing 10 and 15 mg/mL of MNPs (** $p < 0.001$). This finding indicated that both 10 and 15 mg/mL MNPs concentration can be embedded inside the polymeric matrix in order to enhance the adhesion of the H9c2 cells onto the nanofilms. Indeed, the increase of the cell adhesion area was confirmed by incorporating MNPs, as reported in Figure 6f and 6g (representative pictures of 0 and 15 mg/mL, respectively).

Figure 6 about here

The results about the adhesion properties are in agreement with the values found out with the DNA quantification. Taken together, both of the experiments clearly demonstrated that the surface roughness of the magnetic nanofilms, induced by the incorporation of MNPs in different concentrations, improved not only the proliferation but also the adhesion of the H9c2 cells onto these kinds of substrates. Moreover, these findings revealed the significant effects of magnetic nanofilms on H9c2 bioactivities at high concentrations (e.g. 10 mg/mL) of nanoparticles. Similar considerations concerning the effect of nanoparticles-modified surfaces on cellular activities were also found by Lipski *et al.*[32] They demonstrated that the substrates roughness induced by different sizes of nanoparticles had significant effects not only on the proliferation but also on the morphology and cytoskeletal organization of both of the tested cell types (bovine aortic endothelial cells and mouse calvarial preosteoblasts).

The effects of surface wettability on the adhesion of H9c2 cells should be considered. It is well-known that the attachment of cells to various foreign materials is often dictated and controlled by the ability of specific adhesion proteins to adsorb onto their surface; this ability, in turn, depends on the substrates surface properties such as their surface structure, wettability and others. Concerning wettable surfaces, among several researchers Nuttelman *et al.* reported that the maximal cell attachment on polymeric layers occurs on surfaces with moderate contact angles (about 70°-80°).[33] However, protein adsorption and cell adhesion are complex processes, and the basis for this behavior is still poorly understood. Indeed, a good adhesion of H9c2 cells was already achieved at 10 mg/mL of MNPs (97±2°), regardless of the increment of hydrophobicity at 15 mg/mL of MNPs (100±2°). These findings suggest that the surface roughness of the magnetic PLA nanofilms is responsible for the differences in H9c2 cells adhesion, rather than the surface wettability.

Evaluation of nanofilms effects on cell differentiation process. The potential capability of the magnetic PLA nanofilms to induce the differentiation process was explored as the final step of the present study. The morphological study of the differentiated H9c2 was initially assessed through the immunostaining of the cells after 7 days of culture in the specific differentiation medium (1% FBS, 1% ITS). As shown by the qualitative examination, differences in appearance, arrangement and fusion were observed between H9c2 cells cultured on magnetic nanofilms and those cultured on the control ones without MNPs (Figure 7). As a matter of fact, the nanofilms without MNPs showed few fusions of H9c2 (Figure 7a), whereas the samples with MNPs dramatically enhanced myotubes formation supported by the elongation and fusion into multinucleated structures (Figure 7b-d).

In addition, the fusion index and the myotubes area were evaluated as described in Section "*Morphological assessments of differentiated cultures*". The calculated values of these two parameters are reported in Figure 7e and 7f, respectively.

Figure 7 about here

In Figure 7e, the fusion index is reported for each MNPs concentration. The cells incubated with 5, 10, and 15 mg/mL of MNPs presented a non-negligible rise of the fusion index (about 15%), which was statistically different from the control (**$p < 0.001$). However, no significant variations of this parameter were provided among all samples with different concentrations of MNPs. Thus, the increment of the nanofilms surface roughness does not enhance the fusion index of cells seeded on the magnetic substrates. On the contrary, the different surface roughness among the magnetic nanofilms had a significant impact on the surface area of myotubes. A growing trend of the myotubes area (Figure 7f) was followed by cells seeded on the magnetic nanofilms up to 10 mg/mL of MNPs (about 15%, **$p < 0.001$), and statistically significant differences were found between the tested substrates. The statistic between 5 mg/mL and 10 mg/mL of nanoparticles revealed a significant difference between them (**$p < 0.001$). However, although cells seeded on 15 mg/mL of MNPs versus unloaded substrates showed significant differences in the myotubes area (**$p < 0.001$), no significant variations were found between 10 and 15 mg/mL of MNPs. Taking together, these quantitative results suggest that the increment of the roughness has a great impact on the myotube morphogenesis (i.e. it enhances their formation) step wisely up to 10 mg/mL but not 15 mg/mL.

In the field of tissue engineering, there are many efforts to develop polymer-nanoparticles composites, which promote cell proliferation and tissue formation. For example, barium titanate nanoparticles, boron nitride nanotubes, carbon nanofibers can be used to improve the mechanical properties of the cellular scaffolds.[38,40,41] In this regard, due to the specific changes of magnetic nanofilms surface properties in terms of thickness and roughness, MNPs up to 15 mg/mL concentration represent good candidates as structural filler for the reinforcement of the nanofilms. Moreover, with external magnetic fields, the magnetic nanofilms can be manipulated and precisely positioned on the desired place such as the infarcted heart tissue. In addition to these properties, the present study revealed the benefit of MNPs incorporation in the nanofilms; the incremental surface roughness due to MNPs enhanced the morphogenesis of H9c2 cells in both of the adhesion and differentiation processes. Further studies will concern the investigation of cardiomyocyte differentiation into the functional cardiac tissue on the magnetic nanofilms.

CONCLUSIONS

In this study, we investigated the influence of the peculiar structural properties of the magnetic PLA nanofilms on H9c2 cell line activity, showing that their features in terms of surface roughness influenced the cellular morphogenesis. In particular, we revealed how the surface roughness of nanofilms with different concentrations of MNPs affected cytocompatibility, adhesion, proliferation and differentiation of H9c2 cells. The results showed that the incorporation of MNPs into the nanofilms did not compromise the viability of the cells, rather improved both their proliferation and adhesion. Moreover, the differentiation of H9c2 showed the increase of the fusion index and the myotubes area. Collectively, these experimental findings suggest that different surface roughness of the magnetic nanofilms can be obtained by tailoring the content of MNPs loaded in the substrate. The magnetic nanofilms have the potential to realize ultra-thin and flexible structure as a unique tissue engineering scaffold for cardiomyocytes in the field of regenerative medicine.

ACKNOWLEDGMENT

This work was supported in part by JFE (The Japanese Foundation for Research and Promotion of Endoscopy) Grant and JSPS KAKENHI (Grant Number 25870050) from MEXT, Japan (T.F.). The authors would like to thank Mr. Carlo Filippeschi for his support during the clean room activities.

CONFLICT OF INTEREST

No benefit of any kind will be received either directly or indirectly by the authors.

REFERENCES

(1) Khang, D.; Carpenter, J.; Chun, Y. W.; Pareta, R.; Webster, T. J. *Biomed. Microdev.* **2010**, *12*, 575-587.

(2) Jurgens, W. J.; Kroeze, R. J.; Bank, R. A.; Ritt, M. J. P. F.; Helder, M. N. *J. Orthopaed. Res.* **2011**, *29*, 853-860.

(3) Hosseinkhani, H.; Hosseinkhani, M.; Hattori, S.; Matsuoka, R.; Kawaguchi, N. *J. Biomed. Mater. Res. Part A*. **2010**, *94A*, 1-8.

(4) Agrawal, V.; Brown, B. N.; Beattie, A. J.; Gilbert, T. W.; Badylak, S. F. *J. Tissue Eng. Regen. Med.* **2009**, *3*, 590-600.

(5) Jawad, H.; Ali, N. N.; Lyon, A. R.; Chen, Q. Z.; Harding, S. E.; Boccaccini, A. R. *J. Tissue Eng. Regen. Med.* **2007**, *1*, 327-342.

(6) Dalton, B. A.; Walboomers, X. F.; Dziegielewski, M.; Evans, M. D. M.; Taylor, S.; Jansen, J. A.; Steele, J. G. *J. Biomed. Mater. Res.* **2001**, *56*, 195-207.

(7) Lee, S. J.; Khang, G.; Lee, Y. M.; Lee, H. B. *J. Colloid. Interf. Sci.* **2003**, *259*, 228-235.

(8) Bush, J. R. B. J. R.; Nayak, B. K.; Nair, L. S.; Gupta, M. C.; Laurencin, C. T. *J. Biomed. Mater. Res. Part B.* **2011**, *97B*, 299-305.

(9) Raffa, V.; Pensabene, V.; Menciassi, A.; Dario, P. *Biomed. Microdev.* **2007**, *9*, 371-383.

(10) Washburn, N. R.; Yamada, K. M.; Simon, C. G.; Kennedy, S. B.; Amis, E. J. *Biomaterials* **2004**, *25*, 1215-1224.

(11) Stevens, M. M.; George, J. H. *Science* **2005**, *310*, 1135-1138.

(12) Chen C. H.; Chang, Y.; Wang, C. C.; Huang, C. H.; Huang, C. C.; Yeh, Y. C.; Hwang, S. M.; Sung, H. W. *Biomaterials* **2007**, *28*, 4643-4651.

(13) Yeh, Y. C.; Lee, W. Y.; Yu, C. L.; Hwang, S. M.; Chung, M. F.; Hsu, L. W.; Chang, Y.; Lin, W. W.; Tsai, M. S.; Wei, H. J.; Sung, H. W. *Biomaterials* **2010**, *31*, 6444-6453.

(14) Cho, S. W.; Park, H. J.; Ryu, J. H.; Kim, S. H.; Kim, Y. H.; Choi, C. Y.; Lee, M. J.; Kim, J. S.; Jang, I. S.; Kim, D. I.; Kim, B. S. *Biomaterials* **2005**, *26*, 1915-1924.

(15) Piao, H.; Kwon, J. S.; Piao, S.; Sohn, J. H.; Lee, Y. S.; Bae, J. W.; Hwang, K. K.; Kim, D. W.; Jeon, O.; Kim, B. S.; Park, Y. B.; Cho, M. C. *Biomaterials* **2007**, *28*, 641-649.

(16) Fujie, T.; Okamura, Y.; Takeoka, S. *Adv. Mater.* **2007**, *19*, 3549-+.

(17) Forrest, J. A.; Dalnoki-Veress, K.; Stevens, J. R.; Dutcher, J. R. *Phys. Rev. Lett.* **1996**, *77*, 2002-2005.

(18) Fujie, T.; Matsutani, N.; Kinoshita, M.; Okamura, Y.; Saito, A.; Takeoka, S. *Adv. Funct. Mater.* **2009**, *19*, 2560-2568.

(19) Okamura, Y.; Kabata, K.; Kinoshita, M.; Saitoh, D.; Takeoka, S. *Adv. Mater.* **2009**, *21*, 4388-+.

(20) Tang, Z. Y.; Wang, Y.; Podsiadlo, P.; Kotov, N. A. *Adv. Mater.* **2006**, *18*, 3203-3224.

(21) Ai, H.; Jones, S. A.; Lvov, Y. M. *Cell. Biochem. Biophys.* **2003**, *39*, 23-43.

(22) Hammond, P. T. *Adv. Mater.* **2004**, *16*, 1271-1293.

(23) Ricotti, L.; Taccola, S.; Pensabene, V.; Mattoli, V.; Fujie, T.; Takeoka, S.; Menciassi, A.; Dario, P. *Biomed. Microdev.* **2010**, *12*, 809-819.

(24) Pensabene, V.; Taccola, S.; Ricotti, L.; Ciofani, G.; Menciassi, A.; Perut, F.; Salerno, M.; Dario, P.; Baldini, N. *Acta Biomater.* **2011**, *7*, 2883-2891.

(25) Fujie, T.; Ricotti, L.; Desii, A.; Menciassi, A.; Dario, P.; Mattoli, V. *Langmuir* **2011**, *27*, 13173-13182.

(26) Mattoli, V.; Pensabene, V.; Fujie, T.; Taccola, S.; Menciassi, A.; Takeoka, S.; Dario, P. *Proceedings of the Eurosensors XXIII Conference*; Amsterdam, **2009**.

(27) Taccola, S.; Desii, A.; Pensabene, V.; Fujie, T.; Saito, A.; Takeoka, S.; Dario, P.; Menciassi, A.; Mattoli, V. *Langmuir* **2011**, *27*, 5589-5595.

(28) Govoni, M.; Bonavita, F.; Shantz, L. M.; Guarnieri, C.; Giordano, E. *Amino Acids* **2010**, *38*, 541-547.

(29) Ren, K.; Crouzier, T.; Roy, C.; Picart, C. *Adv. Funct. Mater.* **2008**, *18*, 1378-1389.

(30) Zhao, Y.; Marshall, J. S. *Phys. Fluids*. **2008**, *20*, 043302-043302-15.

(31) Xu, C. Y.; Yang, F.; Wang, S.; Ramakrishna, S. *J. Biomed. Mater. Res. Part A*. **2004**, *71A*, 154-161.

(32) Lipski, A. M.; Pino, C. J.; Haselton, F. R.; Chen, I. W.; Shastri, V. P. *Biomaterials* **2008**, *29*, 3836-3846.

(33) Nuttelman, C. R.; Mortisen, D. J.; Henry, S. M.; Anseth, K. S. *J. Biomed. Mater. Res.* **2001**, *57*, 217-223.

(34) Zhang, Q.; Madonna, R.; Shen, W.; Perin, E.; Angeli, F. S.; Murad, F.; Yeh, E.; Buja, L. M.; De Caterina, R.; Willerson, J. T.; Geng, Y. J. *J. Cardiothoracic-Renal Res.* **2006**, *1*, 3-14.

(35) Tryoen-Tóth, P.; Vautier, D.; Haikel, Y.; Voegel, J. C.; Schaaf, P.; Chluba, J.; Ogier, J. *J. Biomed. Mater. Res.* **2002**, *60*, 657-667.

(36) Thierry, B.; Winnik, F. M.; Merhi, Y.; Silver, J.; Tabrizian, M. *Biomacromolecules* **2003**, *4*, 1564-1571.

(37) Hescheler, J.; Meyer, R.; Plant, S.; Krautwurst, D.; Rosenthal, W.; Schultz, G. *Circ. Res.* **1991**, *69*, 1476-1486.

(38) Ciofani, G.; Ricotti, L.; Menciassi, A.; Mattoli, V. *Biomed. Microdev.* **2011**, *13*, 255-266.

(39) Prabhakaran, M. P.; Venugopal, J.; Kai, D.; Ramakrishna, S. *Mater. Sci. Eng. C* **2011**, *31*, 503-513.

(40) Ciofani, G.; Ricotti, L.; Danti, S.; Moscato, S.; Nesti, C.; D'Alessandro, D.; Dinucci, D.; Chiellini, F.; Pietrabissa, A.; Petrini, M.; Menciassi, A. *Int. J. Nanomedicine* **2010**, *5*, 285-298.

(41) Stout, D. A.; Basu, B.; Webster, T. J. *Acta Biomater.* **2011**, *7*, 3101-3112.

(42) Fujie, T.; Okamura, Y. and Takeoka, S. *Functional Polymer Films*, Wiley-VCH Verlag GmbH & Co. KGaA: Weinheim, **2011**, *2*, 907-931.

(43) Shin, H.; Jo, S.; Mikos, A.G. *Biomaterials* **2003**, *24*, 4352–4364.

FIGURE CAPTIONS

Figure 1. Magnetic PLA nanofilms quality assessment. Digital optical microscope images of nanofilms used for the control of their macroscopic morphology with increasing MNPs concentrations: (a) 0 mg/mL; (b) 5 mg/mL; (c) 10 mg/mL; (d) 15 mg/mL. The insets show the presence of nanoparticles clusters with respect to the low (b) and high (d) concentration of MNPs. Scale bars 200 μm (a-d) and 50 μm (insets). (e) A freestanding magnetic nanofilm with the MNPs concentration of 10 mg/mL floating on water surface.

Figure 2. AFM characterization of magnetic PLA nanofilms. Topographical images (scan window 5 μm × 5 μm) for different MNPs concentrations of (a) 0 mg/mL, (b) 5 mg/mL, (c) 10 mg/mL, (d) 15 mg/mL used to measure the surface roughness.

Figure 3. The static sessile drop method to value the hydrophobic properties of the nonmagnetic (a) and magnetic (15 mg/mL) (b) PLA nanofilms. The contact angle is highlighted in red.

Figure 4. Proliferation of H9c2 cells grown on PLA nanofilms loaded with different concentrations of MNPs: (a) 0 mg/mL; (b) 5 mg/mL; (c) 10 mg/mL; (d) 15 mg/mL. LIVE/DEAD fluorescent images show vital cells (green-stained) without apoptotic behavior (red-stained). Scale bar 100 μm.

Figure 5. H9c2 cells after 24 h culture on magnetic PLA nanofilms. Proliferation assay was performed by dsDNA quantification collected from the cell lysates of PLA nanofilms. DNA content as a function of MNPs concentrations. ***$p < 0.001$ at ANOVA test. (N= 9).

Figure 6. Characterization of the H9c2 cells adhesion property on magnetic PLA nanofilms. Cells adhesion behavior on nanofilms with different MNPs concentrations: (a) 0 mg/mL; (b) 5 mg/mL; (c) 10 mg/mL; (d) 15 mg/mL. Immunofluorescence images of cytoskeleton actin (green-

stained) and nuclei (blue-stained) show cells attached to and spread on the nanofilms surface. Scale bar 100 µm. (e) Cells adhesion area as a function of MNPs concentrations. **$p < 0.001$ at ANOVA test. (N=80). (f, g) Representative images of cells adhered on unloaded (0 mg/mL) and loaded (15 mg/mL) PLA nanofilms, respectively. Scale bar 50 µm.

Figure 7. Morphological assessment of H9c2 cells cultured on magnetic PLA nanofilms with different MNPs concentrations: (a) 0 mg/mL; (b) 5 mg/mL; (c) 10 mg/mL; (d) 15 mg/mL. Immunofluorescence staining of nuclei and cytoskeleton actin was performed after 7 days culturing in differentiation medium. Scale bar 100 µm. (e, f) Characterization of the morphology of H9c2 cells cultured on magnetic nanofilms in the differentiation medium after 7 days: (e) fusion index and (f) myotubes area with different concentrations of MNPs. **$p < 0.001$ at ANOVA test. (N=10).

LIST OF TABLES

Table 1. Surface properties of magnetic nanofilms by the function of MNPs concentration.

PLA concentration (mg/mL)	MNPs concentration (mg/mL)	Roughness (nm)	Contact Angle (MEAN±STDEV) (°)	Thickness (MEAN±STDEV) (nm)
20	0	2.54	69±2	147±1
20	5	3.97	79 ±3	193±11
20	10	8.11	97±2	243±11
20	15	18.3	100±2	366±3

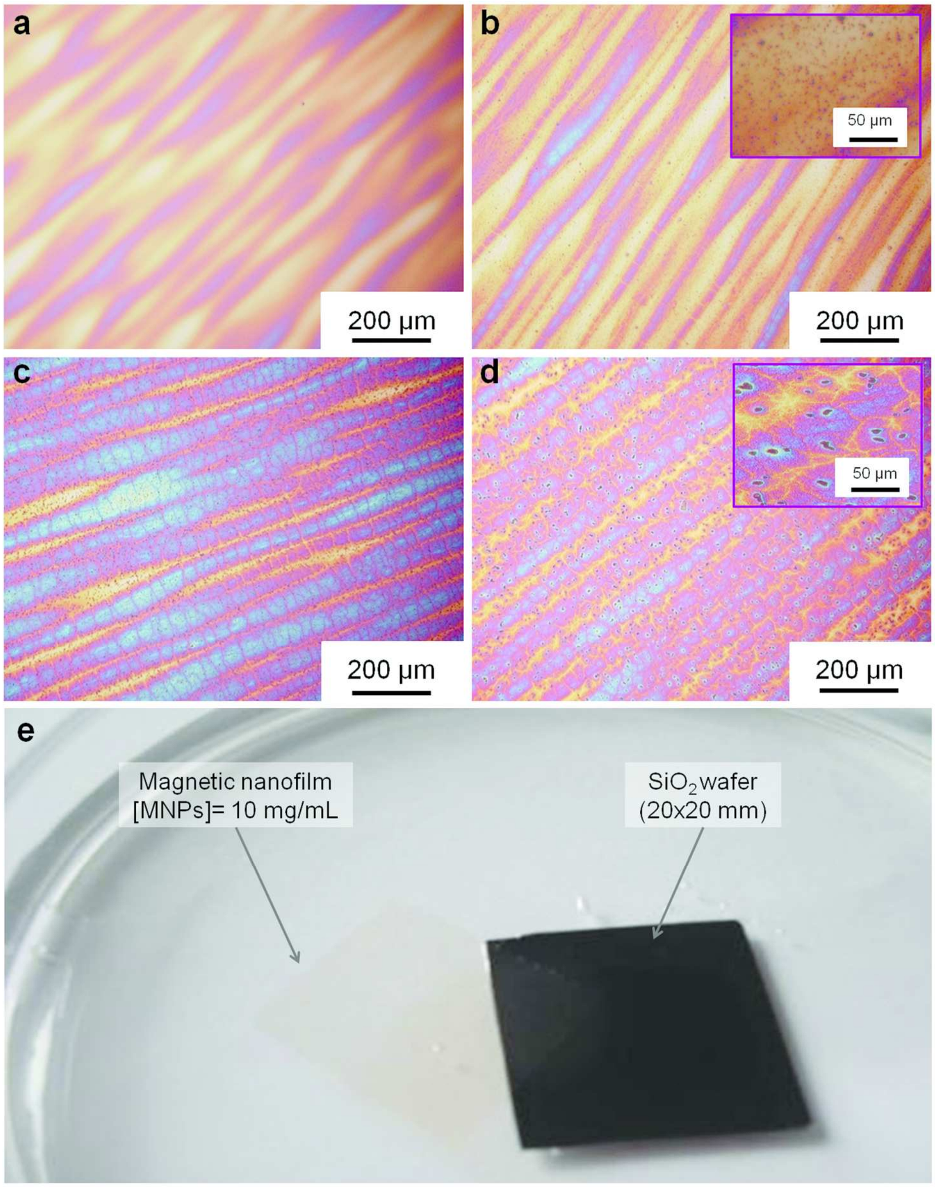

Figure 1. Magnetic PLA nanofilms quality assessment. Digital optical microscope images of nanofilms used for the control of their macroscopic morphology with increasing MNPs concentrations: (a) 0 mg/mL; (b) 5 mg/mL; (c) 10 mg/mL; (d) 15 mg/mL. The insets show the presence of nanoparticles clusters with respect to the low (b) and high (d) concentration of MNPs. Scale bars 200 µm (a-d) and 50 µm (insets). (e) A freestanding magnetic nanofilm with the MNPs concentration of 10 mg/mL floating on water surface.
150x188mm (300 x 300 DPI)

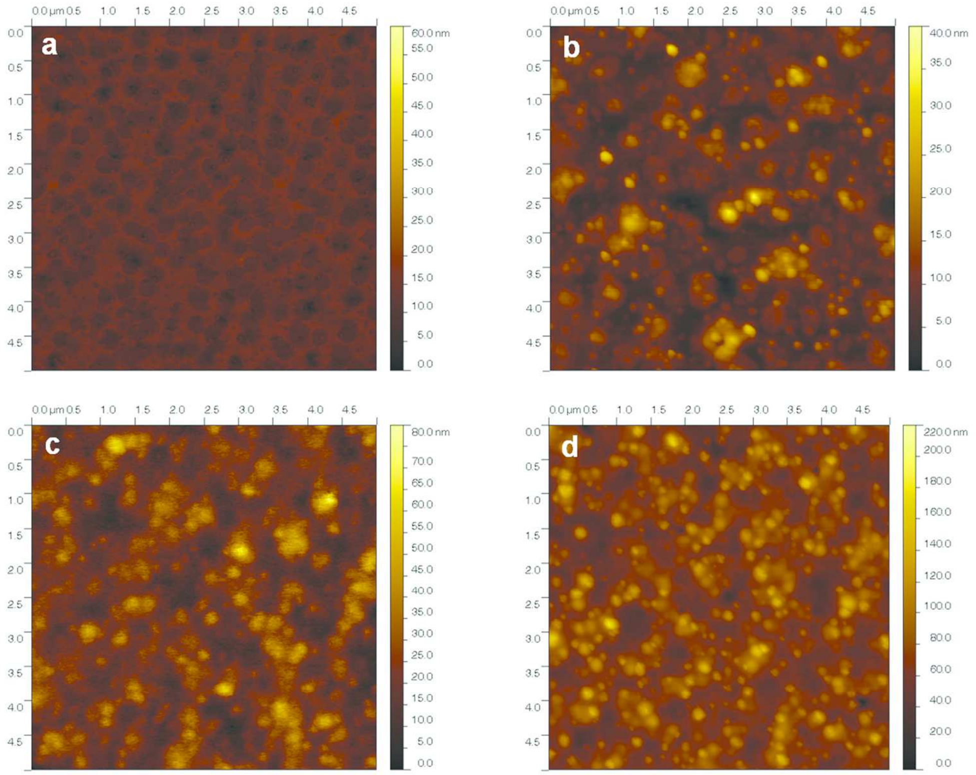

Figure 2. AFM characterization of magnetic PLA nanofilms. Topographical images (scan window 5 µm x 5 µm) for different MNPs concentrations of (a) 0 mg/mL, (b) 5 mg/mL, (c) 10 mg/mL, (d) 15 mg/mL used to measure the surface roughness.
150x120mm (300 x 300 DPI)

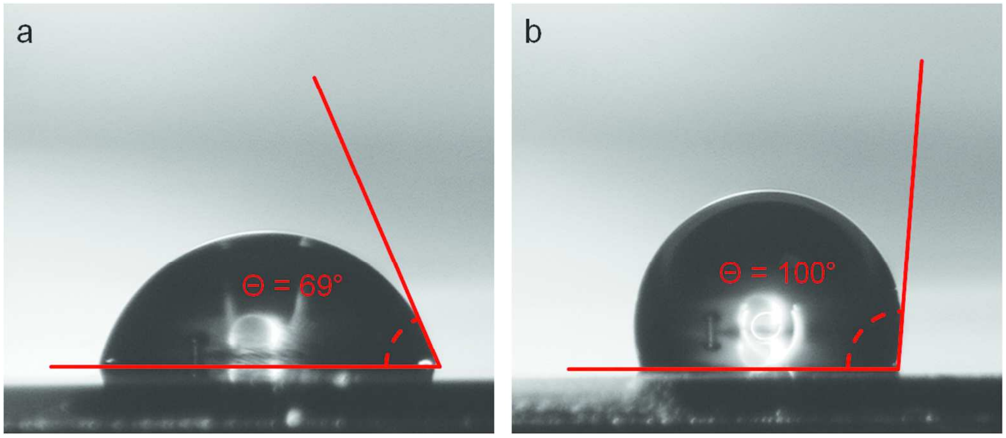

Figure 3. The static sessile drop method to value the hydrophobic properties of the nonmagnetic (a) and magnetic (15 mg/mL) (b) PLA nanofilms. The contact angle is highlighted in red.
150x64mm (300 x 300 DPI)

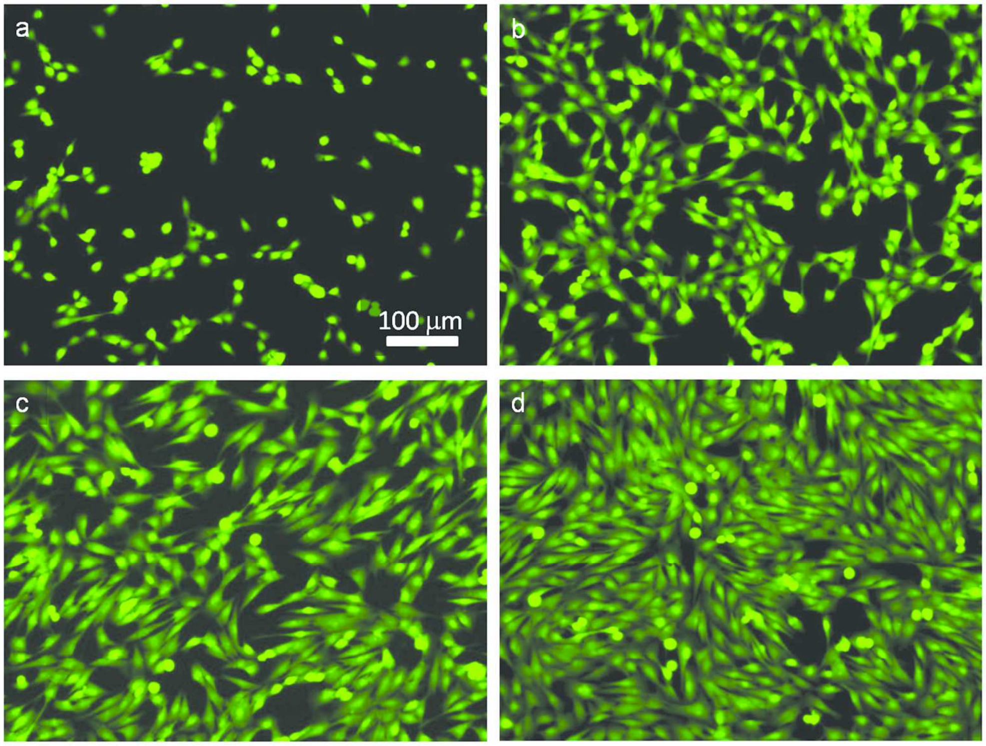

Figure 4. Proliferation of H9c2 cells grown on PLA nanofilms loaded with different concentrations of MNPs: (a) 0 mg/mL; (b) 5 mg/mL; (c) 10 mg/mL; (d) 15 mg/mL. LIVE/DEAD fluorescent images show vital cells (green-stained) without apoptotic behavior (red-stained). Scale bar 100 µm.
150x114mm (300 x 300 DPI)

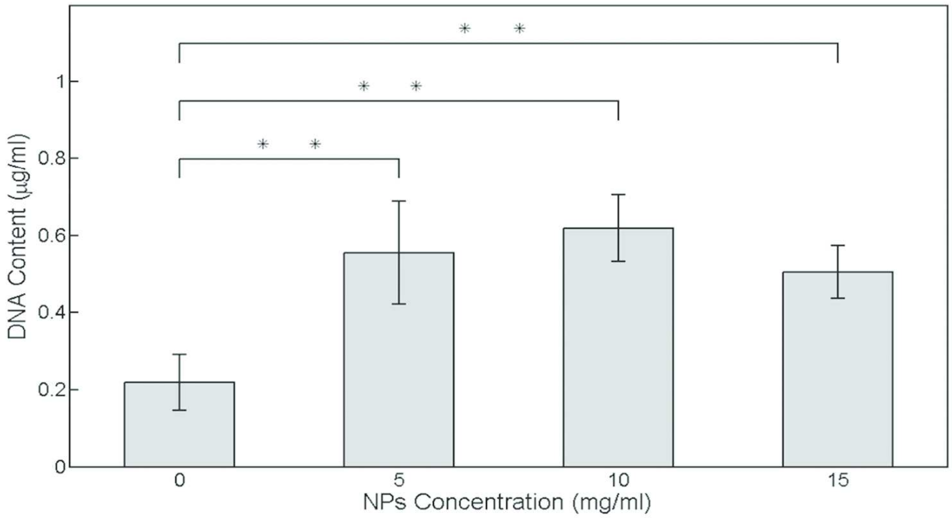

Figure 5. H9c2 cells after 24 h culture on magnetic PLA nanofilms. Proliferation assay was performed by dsDNA quantification collected from the cell lysates of PLA nanofilms. DNA content as a function of MNPs concentrations. Comparison between two groups using the two-tailed Student's t-test (N= 9) with **p < 0.01 set as the level of statistical significance.
150x81mm (300 x 300 DPI)

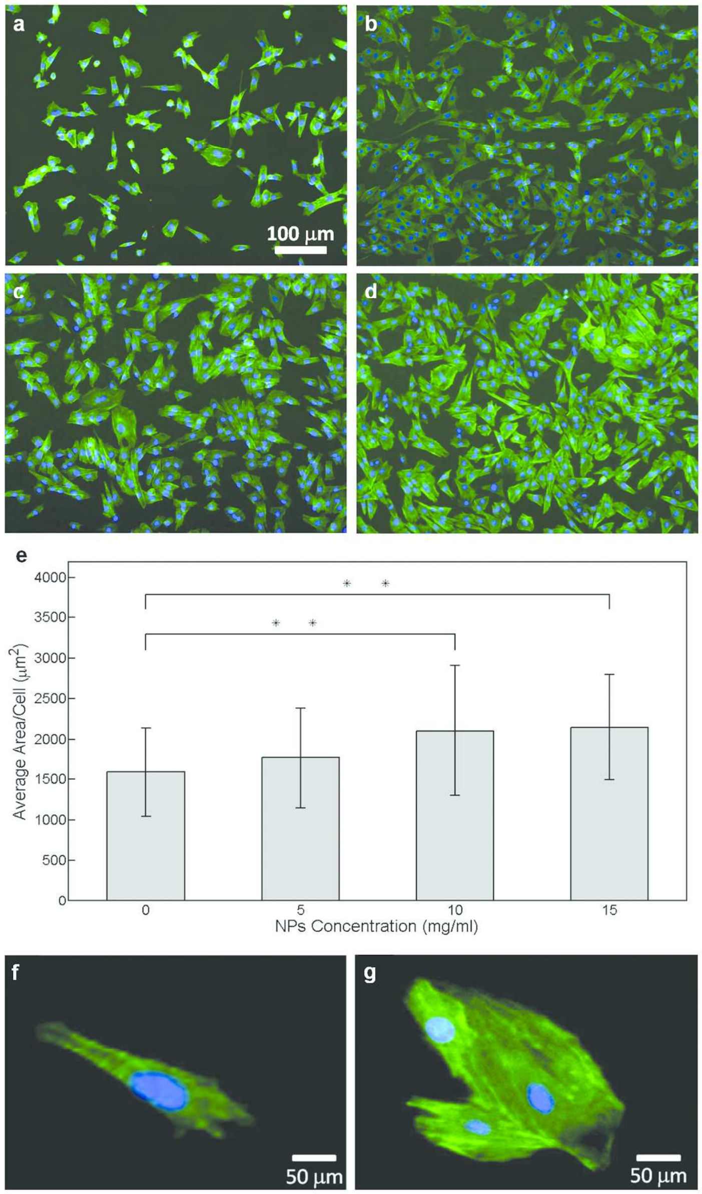

150x252mm (300 x 300 DPI)

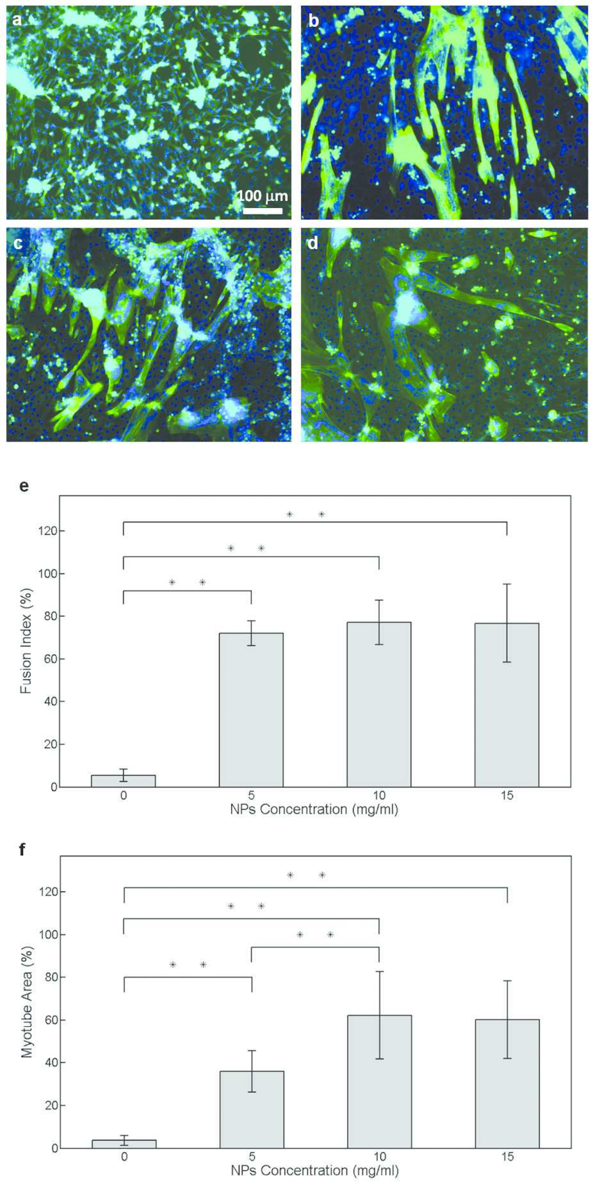

150x302mm (300 x 300 DPI)